

# Embedded plate connection between hollow-core slabs and concrete walls

Kal A. Jackman, Benjamin Z. Dymond, and Brock D. Hedegaard

- This study focuses on end-bearing connections for hollow-core slabs subjected to out-of-plane pressure, out-of-plane suction, and in-plane pressure loading. A new slab-to-wall connection assembly that consisted of a steel plate and stud embedded in the void of a hollow-core slab was investigated.
- An experimental program was run in two phases to determine the capacity of the proposed connection installed in a hollow-core slab (phase 1) and the capacity of the connection for a slab-to-wall subassembly (phase 2). A total of 16 tests were completed for phase 1, and 18 tests were completed for phase 2.
- Test results are compared with predictions using American Concrete Institute's *Building Code Requirements for Structural Concrete (ACI 318-19)* and *Commentary (ACI 318R-19)*, and recommendations are provided based on the experimental results.

A hollow-core slab is a precast, prestressed concrete member with empty voids along its length. Hollow-core slabs are commonly used as floor and roof systems in concrete buildings, parking structures, and other civil structures, which means that they can be subjected to vertical and lateral loads.<sup>1</sup> Both loading scenarios can generate horizontal shear at the connections between hollow-core slabs and their supporting wall elements. However, the hollow-core slab extrusion manufacturing process does not allow for the inclusion of embedded anchors at the time of casting. This means that connection details are often limited to those that can be fabricated after extrusion (when the concrete is not yet cured) or postinstalled during erection. In current practice, hollow-core slabs are connected to the tops of wall elements using doweled or welded connections.

This paper focuses on end-bearing connections for hollow-core slabs, rather than sidelap connections. Shear forces that affect end-bearing connections can be applied in three directions:

- out-of-plane pressure (OP)
- out-of-plane suction (OS)
- in-plane pressure (IP)

Out-of-plane forces are applied perpendicular to the face of the wall, along the longitudinal axis of the hollow-core slab. In this context, pressure refers to an inward force pushing

the anchor into the slab, and suction refers to an outward force pulling the anchor out the end of the slab. In-plane forces are applied in the plane of the wall, transverse to the hollow-core slab, forcing the anchor into an adjacent void. **Figure 1** shows the differences between out-of-plane and in-plane shear forces acting on hollow-core slabs with end-bearing connections to a wall element. Methods to calculate the nominal shear capacity for shear friction are described in American Concrete Institute's *Building Code Requirements for Structural Concrete (ACI 318-19) and Commentary (ACI 318R-19)*.<sup>1</sup> However, there is a lack of experimental data describing the horizontal shear capacity of the hollow-core slab connection.

## Background for current precast concrete slab-to-wall connections

The two most common slab-to-wall connections currently used in the U.S. precast concrete industry are dowel connections and welded steel angle connections. A dowel connection is commonly made between two precast concrete elements using a straight piece of steel reinforcement and is a common solution to transfer horizontal shear forces. While the connection is simple, the behavior can be complex and is influenced by the behavior of different materials (concrete and steel), contact between elements (for example, beam to column and floor to wall), and fixity of the connection (for example, pinned or rigid).<sup>2</sup> There are various possible failure modes associated with dowel connections:<sup>3</sup>

- steel shear failure
- concrete splitting failure
- steel flexural failure

Steel shear failure occurs when the bar experiences a shear load that causes fracture across the shear plane. Concrete splitting failure occurs when the shear force displaces the dowel, creating a high concentrated force in the concrete, which causes the

concrete to crack and split. Steel flexural failure is a combination of steel shear failure and concrete splitting failure.

A typical dowel connection consists of a postinstalled no. 4 (13M) reinforcing bar that goes through the hollow-core slab into the supporting wall, which can be made of cast-in-place concrete, precast concrete, or concrete masonry units with a bond beam (**Fig. 2**). In this connection, hollow-core slabs can span perpendicular to the wall (end bearing) or parallel to the wall (sidelap) to resist horizontal shear forces. The dowel installation process consists of drilling a hole through the hollow-core into the wall; the drilled hole diameter is the same as the dowel diameter. The dowel is then placed into the predrilled hole, creating the force-fit dowel connection. This dowel connection is frequently used because it is simple, transfers diaphragm shear, and provides lateral wall bracing. However, the connection capacity must be verified by testing.<sup>4</sup> Previous research by the Spancrete Manufacturers' Association (SMA)<sup>5</sup> investigated a limited number of these cost-effective connections between one size and cross section of a hollow-core slab and a masonry bond beam. The SMA reported three shear capacity values (OP, OS, and IP) for both the end-bearing and sidelap conditions (**Table 1**). Their research arrived at the following conclusions:

- The shear force was transferred through the connection.
- The thickness of the hollow-core slab did not affect the capacity of the connection.
- The thickness of concrete below the cores was the minimum thickness in use in 2010, and the results can therefore be applied to other slab cross sections.
- A strength-reduction factor of 0.7 is appropriate based on the results from a small number of samples.

Brito et al.<sup>6</sup> analyzed a keyway connection, which is like the dowel connection. This connection utilized a no. 3 (10M)

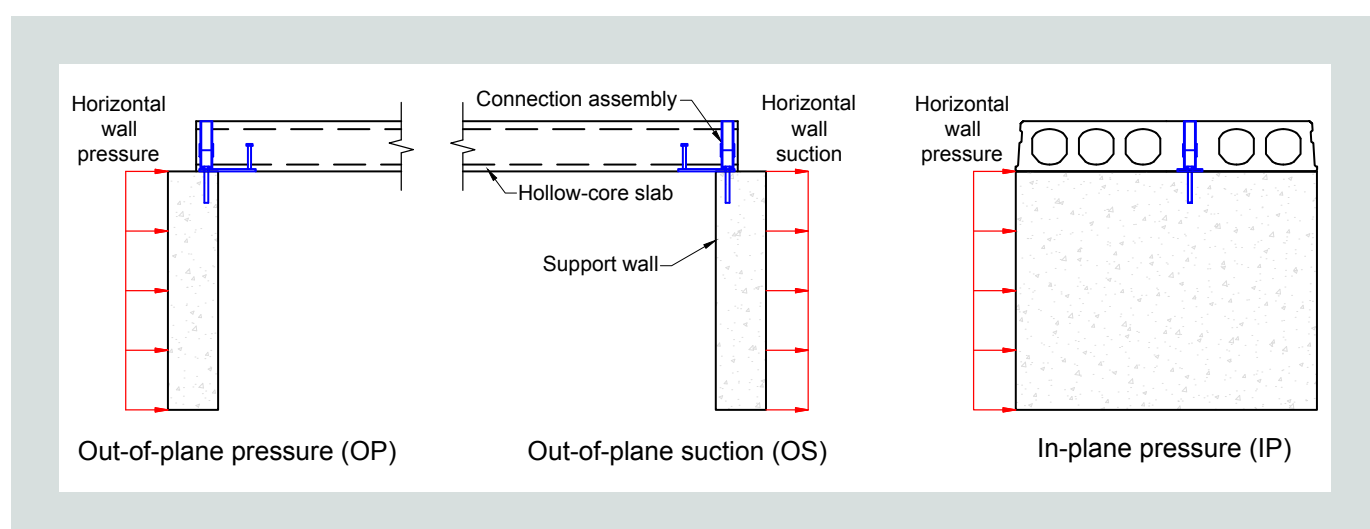


**Figure 1.** Horizontal wall loading applied to a slab-to-wall connection assembly resulting in out-of-plane pressure, out-of-plane suction, and in-plane pressure.

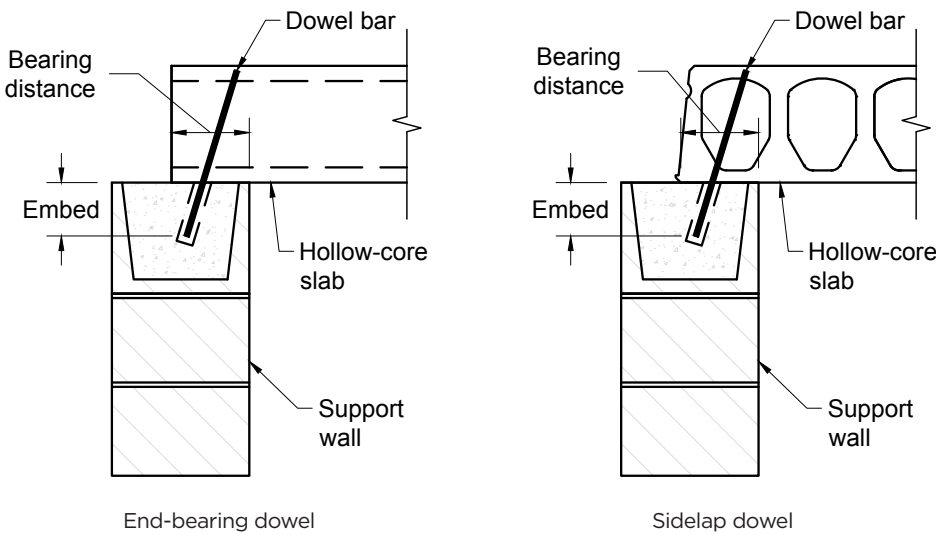


**Figure 2.** Elevation view of an end-bearing and sidelap dowel connection between a hollow-core slab and supporting wall element.

**Table 1.** End-bearing and sidelap dowel connection results reported by Spancrete Manufacturers' Association for OP, OS, and IP loading

Bearing condition	Loading direction	Minimum experimental failure load, kip	Failure mode
End bearing	OP	3.40	Concrete cone
	OS	2.78	Concrete cone
	IP	4.50	Reinforcing bar yield
Sidelap	OP	2.96	Bond beam spalling
	OS	1.87	Bond beam spalling
	IP	2.66	Bond beam spalling

Source: Data from Spancrete Manufacturers' Association (2010).

Note: IP = in-plane pressure; OP = out-of-plane pressure; OS = out-of-plane suction.

1 kip = 4.448 kN.

reinforcing bar bent at 90 degrees as a dowel to connect hollow-core slabs to concrete masonry unit support walls. The concrete masonry unit support walls were 7.5 in. (190 mm) wide and topped with a U-shaped bond beam that contained two no. 3 steel reinforcing bars. To complete the end-bearing connection, a hole was predrilled in the wall and vacuumed. The 90-degree bent bar was hammered into the hole with or without an epoxy adhesive, and these conditions were identified as adhesive or dry fit, respectively. A hollow-core slab was placed on each side of the dowel, creating the keyway that surrounds the reinforcing bar. The connection was completed by grouting the keyway between the two hollow-core slabs, thus encapsulating the reinforcing bar (Fig. 3). Brito et al.<sup>6</sup> reported three peak load values (OP, OS, and IP) for both the end-bearing and sidelap conditions (Table 2). Their research arrived at the following conclusions:

- The direction of loading influenced the way the connection failed.
- The longitudinal bars in the concrete masonry unit wall contributed to the ductile behavior of the connection.

Welded steel angle connections (Fig. 4) are the other most common type of slab-to-wall connection used in the U.S. precast concrete industry. Typically, this connection consists of a steel angle attached to the wall element, a steel plate in the hollow-core slab, and a field weld connecting the two elements. There are two ways the steel angle is attached to a precast or cast-in-place concrete wall:

- The angle is welded to an embed plate installed in the wall.

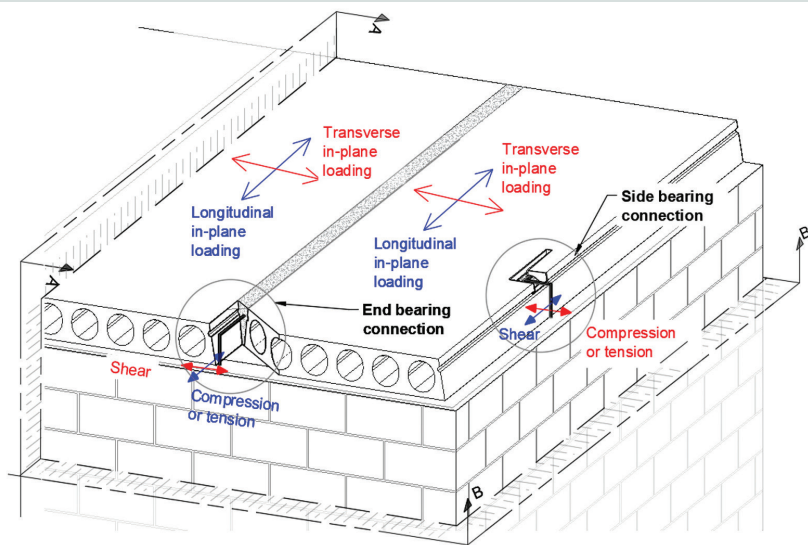


**Figure 3.** End-bearing connection between hollow-core slabs and a masonry wall, made with a reinforcing bar in the shear key. Source: Reproduced by permission from Brito et al. (2022), Fig. 1, page 53.

**Table 2.** End-bearing and sidelap keyway connection results reported by Brito et al. for OP, OS, and IP loading

Bearing condition	Loading direction	Peak experimental load, kip	Failure mode
End bearing	OP	5.6	Bar pullout, yielding, and bond beam fracture
	OS	2.1	Bar cover spalling, bar pullout, and loss of bearing
	IP	5.8	Bar yielding and pullout
Sidelap	OP	4.8	Bar pullout, yielding, and beam crushing
	OS	2.0	Bar pullout and loss of bearing
	IP	1.8	Bar yielding and pullout

Source: Data from Brito et al. (2022).

Note: IP = in-plane pressure; OP = out-of-plane pressure; OS = out-of-plane suction. 1 kip = 4.448 kN.

- The angle is attached using a postinstalled anchor, typically screw anchors or expansion anchors.

In concrete masonry unit walls, the angle is typically attached using postinstalled screw anchors. To embed a plate in the hollow-core slab, a plate with headed studs or deformed bar anchors is situated in one of the hollow voids after extrusion and the void is backfilled with concrete to secure the embedded plate. On-site, the hollow-core embed plate is welded to the angle attached to the wall. The strength of the welded connection is based on four components:

- postinstalled anchors (if applicable)
- embedded plate
- angle
- weld

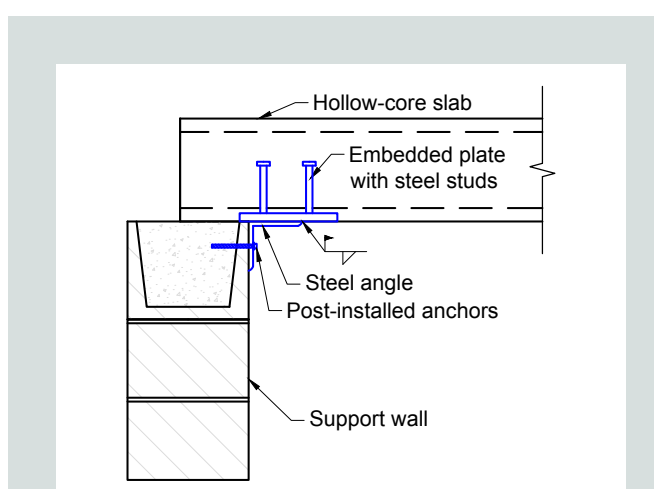


**Figure 4.** Elevation view of a typical welded steel angle connection.

## Investigated embedded steel plate and stud slab-to-wall connection assembly

This research program investigated a new end-bearing slab-to-wall connection assembly that consisted of an embedded

steel plate and stud, as shown in **Fig. 5** and **6**. The connection assembly included a 4 by 9 in. (102 by 229 mm) Grade A36 steel plate with a 0.5 in. (12.7 mm) diameter shear stud. The plate also had a predrilled hole, meant to accept a postinstalled screw anchor, surrounded by a steel

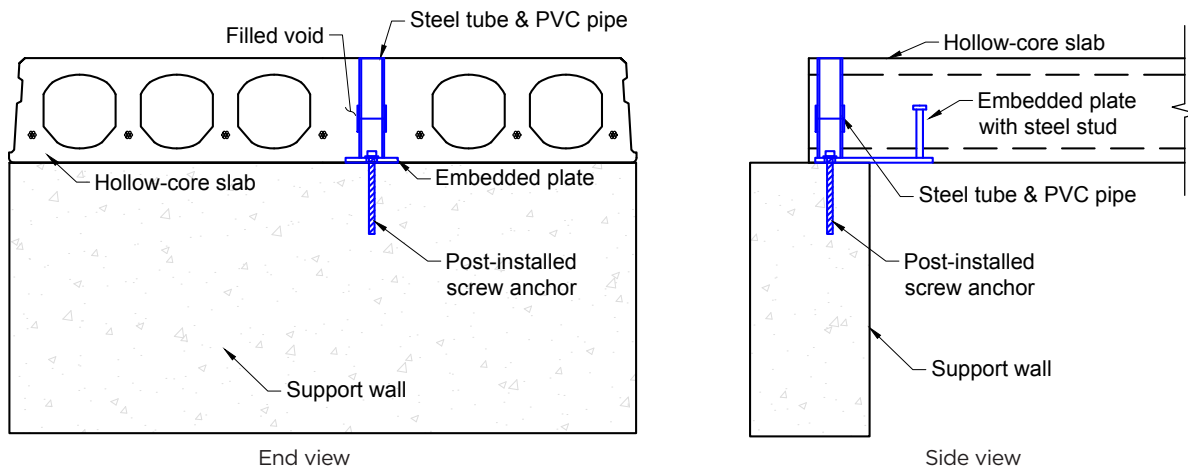


**Figure 5.** The investigated embedded steel plate and stud connection between a hollow-core slab and support wall, shown from an end view and side view. Note: PVC = polyvinyl chloride.

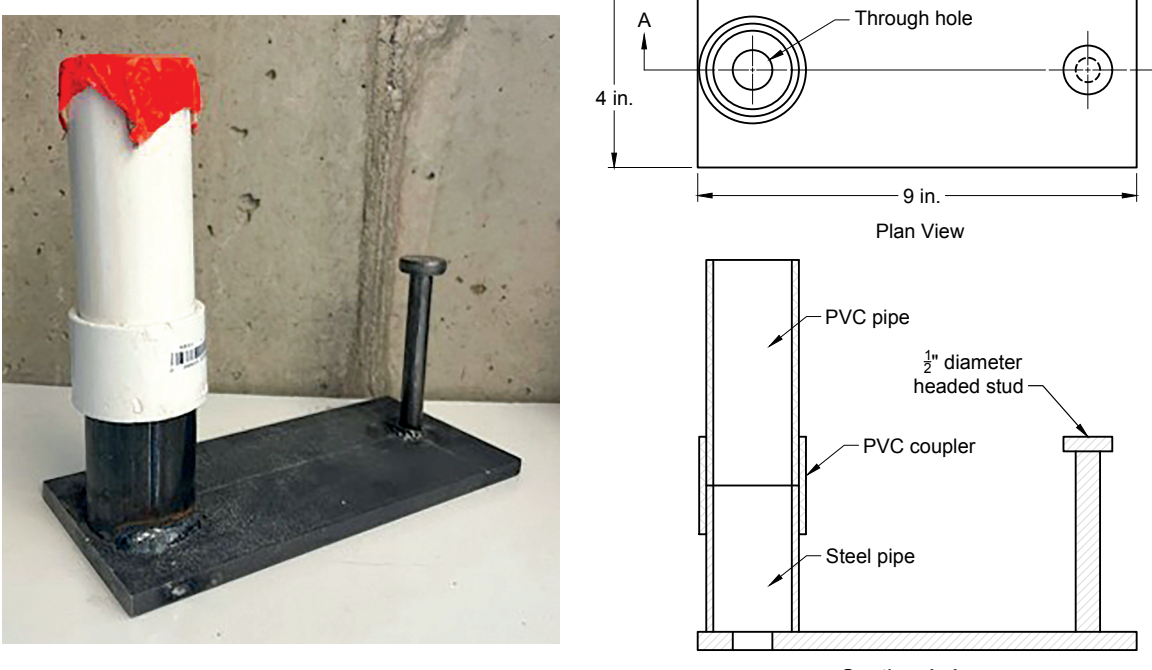


**Figure 6.** Embedded steel plate and stud connection assembly investigated in this research program. Note: PVC = polyvinyl chloride; 1 in. = 25.4 mm.

tube welded to the embed plate on two sides. In addition, a polyvinyl chloride (PVC) pipe was coupled to the steel tube so the height of the system matched the 8 in. (203 mm) height of the hollow-core slab.

Because of the manufacturing process, the embedded plate and stud assembly was installed into a void in the hollow-core slab after extrusion (Fig. 7), as follows:

1. The locations where the embedded steel plate and stud connection hardware should be installed were marked on the top face of the extruded slab, above empty voids.
2. At each marked location, the top and bottom flange were removed, creating an empty region for the embedded steel plate and stud connection hardware.
3. The embedded plate and stud assembly was placed within the empty region such that the flat portion of the embedded plate sat on the formwork bed.
4. The region of the hollow-core void in which the embedded plate was installed was backfilled with concrete, which bonded the embedded plate and stud to the hollow-core slab. The bottom surface of the embedded plate and the top edge of the PVC pipe remained exposed on the bottom and top sides of the slab, respectively.

Coupling the PVC pipe to the steel tube allowed access to the predrilled hole in the embedded plate, which in turn facilitated easy installation of a postinstalled screw anchor in the field. For this research program, a 0.625 in. (16 mm) diameter hole was drilled in the wall using the access provided by the steel tube and PVC pipe. The hole depth of 7 in. (178 mm) was selected based on the required embedment length of the screw plus an additional 2 in. (51 mm) to allow for settling of concrete dust from the drilling process. After drilling, the hole was vacuumed clean and the screw anchor was installed to secure the hollow-core slab to the wall. If desired, the PVC hole could be filled with grout to achieve a flat finished surface.

There are three distinct benefits of using this embedded steel plate and stud connection compared with existing types of connections. First, the field assembly of the connection is simple. The proposed connection only requires drilling a hole and installing a screw anchor. The connection does not depend on field welding, which is a requirement of welded steel angle connections. Second, the screw anchor capacity and support wall concrete breakout capacity are the only aspects of the connection that require design. The strength of the embedded plate and stud assembly is intended to have higher capacity than the anchor and supporting concrete; this was verified in the testing described herein. Third, this proposed connection is less sensitive to construction errors and misalignment because it is premanufactured in the controlled environment of a precasting plant rather than at the jobsite.



Backfilling of void and flanges with concrete  
Embedded connection assembly sitting on formwork bed with top of PVC exposed  
Area with removed top and bottom flanges

**Figure 7.** Step 4 in the embedded plate and stud installation process, where the void and removed flanges are backfilled after inserting the hardware. The flat portion of the embedded plate is sitting on the formwork bed, and the top of the polyvinyl chloride (PVC) pipe remains exposed on the top side of the slab.

## Research objectives

The main goal of this study was to experimentally evaluate the strength of the concrete surrounding the investigated embedded steel plate and stud connection assembly with a desired outcome that the steel connection assembly would have more capacity than the surrounding concrete. The research objectives were as follows:

- Experimentally determine the capacity of the proposed connection for an assembly installed in a hollow-core slab subjected to OP, OS, and IP loading.
- Experimentally investigate the behavior and capacity of the connection when subjecting an end-bearing slab-to-wall subassembly to OP, OS, and IP loading.
- Compare observed failure modes and loads with those predicted using ACI 318<sup>1</sup> and reported in the literature.

## Experimental program and methods

### Scope of testing

**Table 3** lists the variables investigated in the experimental program, delineated in two phases, referred to as P1 and P2 in the experimental nomenclature. The objective of phase 1 was to determine the capacity of the proposed connection when an assembly installed in a hollow-core slab was subjected to OP, OS, or IP loading. Specimens subjected to OS loading had assemblies that included either a 0.5 or 0.75 in. (12.7 or 19 mm) headed stud. Four specimens with each of the headed stud diameters were tested (eight total). Specimens

subjected to OP and IP loading had an embedded plate with a 0.5 in. headed stud, and four tests were conducted in each direction. Thus, a total of 16 tests were completed in phase 1. The objective of phase 2 was to determine the capacity of the connection when subjecting a slab-to-wall subassembly to OP, OS, or IP loading. Two types of walls were tested in subassemblies: cast-in-place walls with or without confinement reinforcement. This reinforcement was located at the top of the wall, near the location of the connection between the hollow-core slab and wall. Phase 2 consisted of a total of eighteen tests, nine conducted using walls with confinement reinforcement (R) and nine conducted using unreinforced (UR) walls (without confinement reinforcement). The naming convention of each specimen was delineated by phase (P1, P2), type of support cast-in-place wall for phase 2 (UR, R), loading direction (OP, OS, IP), and test number (1 to 4). For example, the fourth specimen tested in phase 1 using IP loading was designated P1-IP-4.

The nominal bearing length of the hollow-core slab sitting on top of the cast-in-place wall was 5.5 in. (140 mm) for the wall with confinement reinforcement and 3.5 in. (89 mm) for the wall without confinement reinforcement. The edge distances reported in Table 3 represent the average distance from the center of the screw anchor to the outside edge, inside edge, or nearest side edge of the wall for OP, OS, and IP loading, respectively; this distance was used for wall concrete breakout calculations. The slab was positioned on the wall to ensure this edge distance was consistent among the three repeated tests for each test case. Thus, because of minor variations in the placement of the embedded plate assembly within the hollow-core slab, the nominal bearing distance was different for each test to achieve this consistent edge distance.

**Table 3.** Variables investigated in the experimental program, delineated in two phases

Phase	Test type	Loading direction	Stud diameter, in.	Nominal bearing length, in.	Edge distance, in.	Specimen naming	Number of tests
P1	Capacity of embedded plate and stud assembly	OP	0.5	n/a	n/a	P1-OP	4
		OS	0.5			P1-OS	4
		OS	0.75			P1-OS-3/4	4
		IP	0.5			P1-IP	4
P2	Slab-to-wall subassembly with unreinforced cast-in-place walls	OP	0.5	3.5	4.708	P2-UR-OP	3
		OS	0.5		1.917	P2-UR-OS	3
		IP	0.5		2.375	P2-UR-IP	3
	Slab-to-wall subassembly with reinforced cast-in-place walls	OP	0.5	5.5	2.042	P2-R-OP	3
		OS	0.5		4.5	P2-R-OS	3
		IP	0.5		3.75	P2-R-IP	3
Total							34

Note: IP = in-plane pressure; n/a = not applicable; OP = out-of-plane pressure; OS = out-of-plane suction; P1 = phase one; P2 = phase 2; R = reinforced; UR = unreinforced. 1 in. = 25.4 mm.

## Hollow-core slab properties

The extruded (dry-cast) normalweight hollow-core slabs tested as part of this program were 8 in. (200 mm) thick and contained seven 0.5 in. (12.7 mm) diameter low-relaxation 270 ksi (1860 MPa) prestressing strands. The specified 28-day hollow-core concrete compressive strength was 9000 psi (62.1 MPa). The slab cross section is shown in **Fig. 8**. The investigated connection assembly was installed in an interior void that was backfilled. The final cross-sectional width of the hollow-core slabs varied based on the phase and testing setup. Phase 1 used a full slab width of 4 ft (1.2 m) for the OP tests and a saw-cut width of 3.38 ft (1.0 m) for the IP test. All tests in phase 2 used a saw-cut slab with a width of 3.38 ft (1.0 m). Lengths of the hollow-core slabs varied based on the phase and testing setup (**Table 4**).

## Cast-in-place wall properties

The geometry of the normalweight cast-in-place walls used during subassembly testing (**Fig. 9**) varied based on the test setup geometry and direction of loading. All walls were 8 in. (200 mm) thick. The wall height was 3.17 ft (0.97 m) for OP and OS loading or 1.31 ft (0.4 m) for IP loading. The wall length was either 6 or 11.5 ft (1.8 or 3.5 m) depending on the test setup geometry. All cast-in-place wall sections had either D7.5 wire mesh or longitudinal no. 4 (13M) reinforcing bars in the bottom of the cross section to prevent cracking during lifting and shipping. The walls without confinement reinforcement did not have reinforcement in the top 10 in. (254 mm) for OP and OS loading or 6.5 in. (165 mm) for IP loading, whereas walls with confinement reinforcement had continuous D7.5 wire mesh throughout the cross section. The specified 28-day concrete compressive strength for the cast-in-place walls was 5000 psi (34.5 MPa), and the measured compressive strength ranged from 5100 to 5800 psi (35.1 to 40 MPa) at the time of testing.

## Test setups and procedures

In phase 1, load was applied directly to the proposed connection assembly installed in a hollow-core slab. A representative

example of the phase 1 test setup and the testing orientations for OP, OS, and IP loading scenarios is shown in **Fig. 10**. The general test setup included a vertical hollow-core slab that was secured to a strong floor. A built-up steel T shape was used to connect the embedded plate to an actuator. The T shape consisted of a 1 in. (25.4 mm) thick base plate attached to the actuator with a vertical C3×5 channel and steel plate welded together and extending down from the actuator. The vertical channel and plate had three predrilled holes that were used to attach the hollow-core slab connection assembly to the actuator based on the loading direction. The actuator was attached to the connection assembly using a 0.75 in. (19 mm) A325 bolt, which was assumed to have an unfactored shear capacity of 23 kip (102 kN).<sup>7</sup> The actuator pulled upward at a rate of approximately 0.0001 in./sec (0.00254 mm/sec) to apply force to the installed connection assembly.

Representative examples of the phase 2 test setup are shown in **Fig. 11**. The long supporting walls were designed to have multiple locations for testing along the length (for example, one wall had three testing sites), where the proposed connection assembly embedded in a hollow-core slab was attached to the wall with a screw anchor. This decreased the number of walls required for testing. OP loading pushes on the exterior of the wall, parallel to the length of the voids in the hollow-core, and OS loading pulls outward on the wall (Fig. 1). To mimic OP and OS loading, lateral force was applied to the hollow-core slab, which was the moving component, parallel to the direc-

**Table 4.** Length of the hollow-core specimen used for testing

Testing direction	Phase 1, ft	Phase 2, ft	
		Unreinforced	Reinforced
OP	4.0	4.0	4.17
OS	4.0	5.33	5.5
IP	4.0	4.0	4.0

Note: IP = in-plane pressure; OP = out-of-plane pressure; OS = out-of-plane suction. 1 ft = 0.305 m.

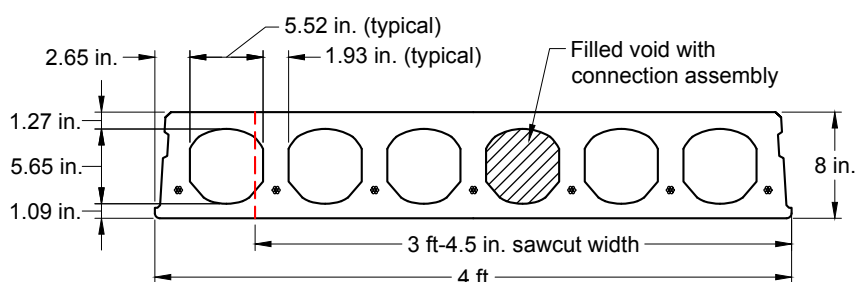


**Figure 8.** Cross section of the hollow-core slab with annotation to show where specimens were saw cut along the width and which void was backfilled with concrete surrounding the installed embedded steel plate and stud connection assembly. Note: 1 in. = 25.4 mm.

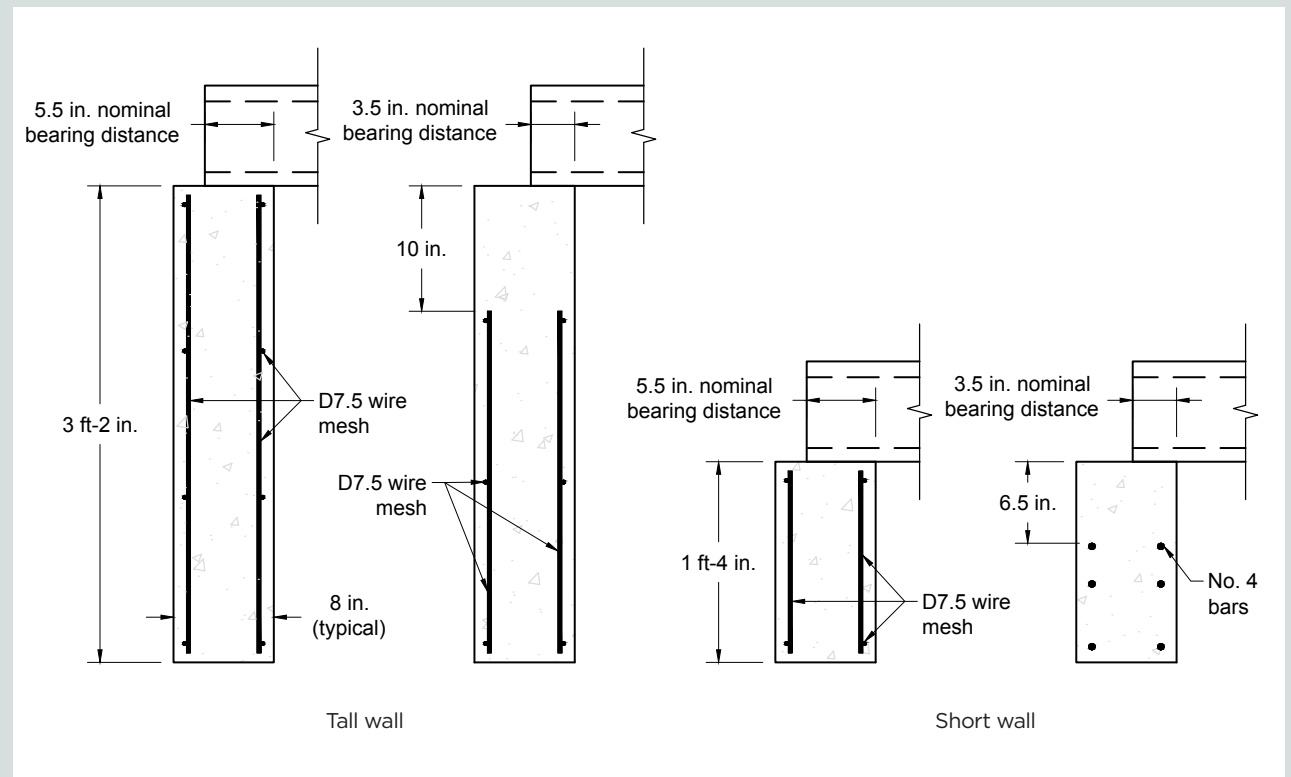


**Figure 9.** Tall wall cross sections with and without confinement reinforcement and short wall sections with and without confinement reinforcement. Note: No. 4 = 13M. 1 in. = 25.4 mm.

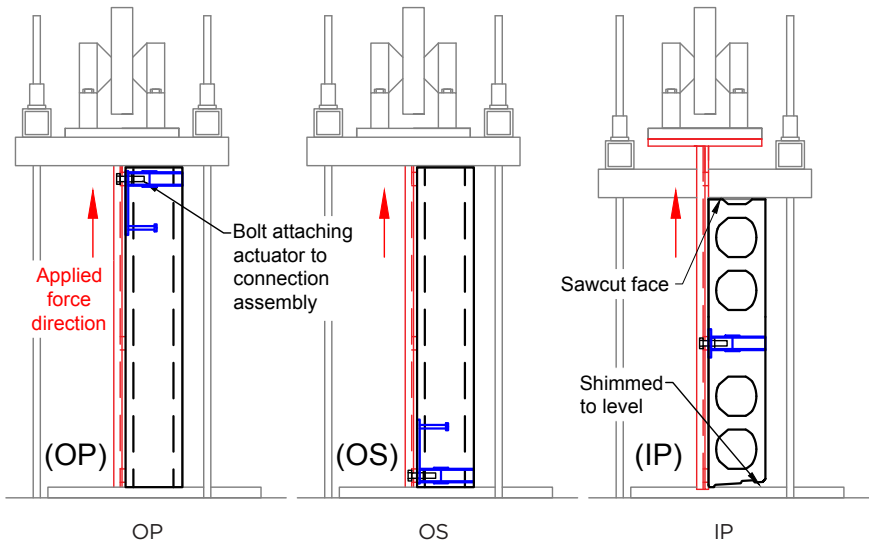


**Figure 10.** Representative phase 1 test setup and cross-sectional views of the hollow-core slab orientation to generate out-of-plane pressure, out-of-plane suction, and in-plane pressure loading. Note: IP = in-plane pressure; OP = out-of-plane pressure; OS = out-of-plane suction;

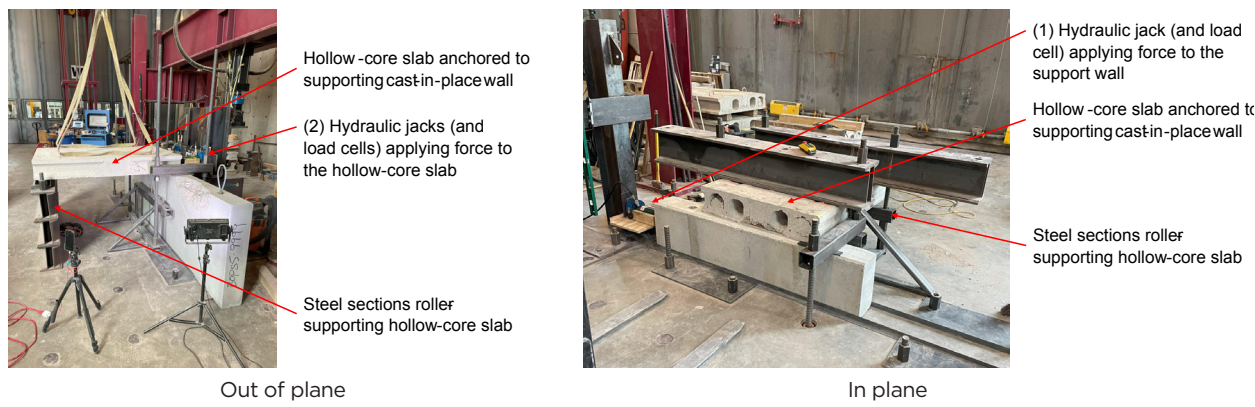


**Figure 11.** Representative phase 2 test setups for out-of-plane pressure and out-of-plane suction testing and in-plane pressure testing.

tion of the voids using two hydraulic jacks (Fig. 12). IP loading pushes parallel to the wall, perpendicular to the length of the voids in the hollow-core (Fig. 1). To mimic IP loading, lateral force was applied to the short wall section, which was the moving component, using a single hydraulic jack (Fig. 12). To minimize the friction force between the short wall and the floor, two rows of stacked multipolymer plastic pads were placed on the outside edges of the bottom of the wall between the floor and wall. Other than the self-weight of the hollow-core slabs, no additional loading was applied in the vertical direction in all tests. Applied force data were recorded over time using load cells positioned between the hydraulic jack(s) and the moving concrete component in each test setup. Additional specific details related to the test setups, hollow-core slab lengths, and cast-in-place wall lengths were published by Jackman.<sup>8</sup>

## Experimental failure modes and capacity results

### Phase 1 connection assembly failure modes

During OP testing, where the connection assembly was forced into the slab, none of the specimens experienced concrete

failure. Instead, two of the tests ended when the A325 bolt attaching the connection assembly to the actuator failed in shear (P1-OP-2 and P1-OP-3), and two of the tests ended when the embedded plate and stud connection assembly failed (P1-OP-1 and P1-OP-4). Failure of the connection assembly was characterized by initial fracture of the weld connecting the steel tube to the plate. Concrete deformation during testing caused the tube to bend and no longer be perpendicular to the plate. Following deformation of the tube, the base of the steel stud sheared, leading to failure. The weld fracture, tube deformation, and sheared stud are shown in Fig. 13. As the connection assembly failure occurred, the applied force caused the front face of the hollow-core slab to spall off.

During testing of all OS specimens with a 0.5 in. (12.7 mm) headed stud, failure began with concrete spalling at the front face of the hollow-core slab and ended with shearing of the headed stud (Fig. 14). Because the goal of this research project was to create a steel connection assembly that had more capacity than the surrounding concrete, the set of four P-OS-3/4 specimens were constructed with a 0.75 in. (19 mm) diameter stud to change the expected failure mechanism to a concrete breakout. The failure mode for all four tests with the 0.75 in. headed studs was a triangular concrete breakout section that

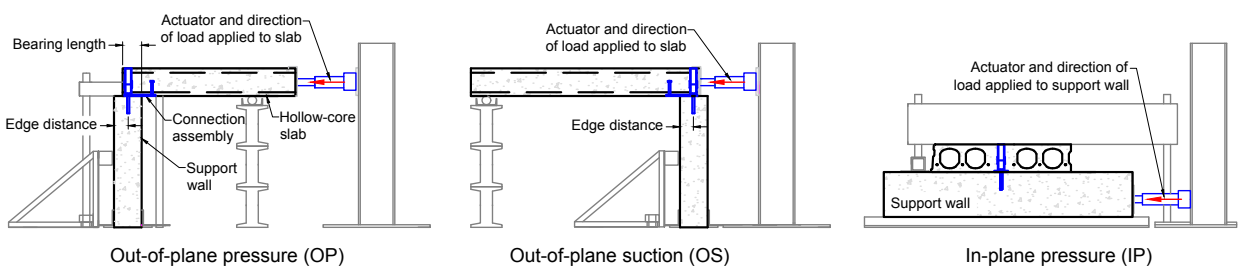


**Figure 12.** Cross-sectional drawings of the test setups.

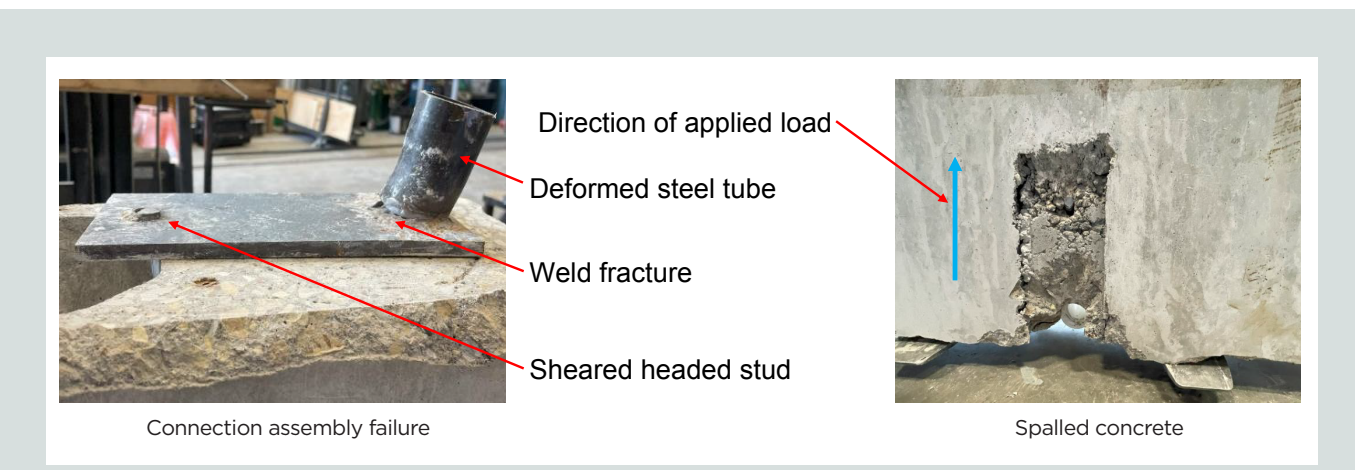


**Figure 13.** Connection assembly failure during phase 1 out-of-plane pressure testing via weld fracture, tube deformation, and stud shearing that led to spalled concrete at the front face of the hollow-core slab.

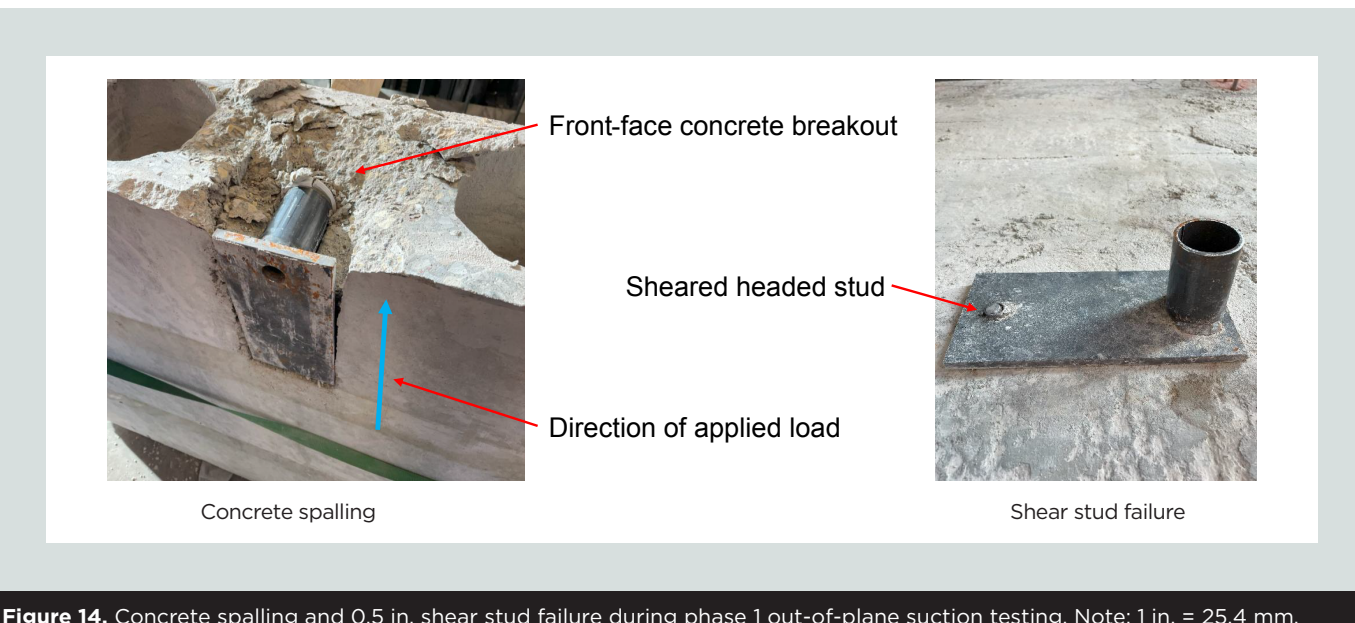


**Figure 14.** Concrete spalling and 0.5 in. shear stud failure during phase 1 out-of-plane suction testing. Note: 1 in. = 25.4 mm.

centered around the embedded plate (Fig. 15). The angle of each side of the concrete breakout section was measured and ranged from 20 to 29.5 degrees; the angle of the breakout section was estimated to be 35 degrees using ACI 318-19,<sup>1</sup> but that estimation was for a solid block of concrete and not a hollow-core section with voids. Failure cracking propagated on the bottom flange from the triangular breakout section along the length of the void that contained the filled core (Fig. 15).

During IP testing, the force applied to the embedded plate was perpendicular to its length and not centered on the plate but rather centered on the tube through which the slab-to-wall connection would be made, which created eccentric loading. The failure of all IP specimens was characterized by rotation of the embedded plate and steel tube about the point of the steel stud. As the connection assembly rotated upward, the front and bottom faces of the hollow-core slab cracked and began to spall; sudden failure was triggered by brittle cracking of the plastic PVC pipe coupler. The failure mode is illustrated in Fig. 16.

## Phase 2 slab-to-wall subassembly failure modes

During all phase 2 testing, the subassemblies failed due to concrete breakout of the cast-in-place support wall (Fig. 17). No damage to the embedded plate and stud or postinstalled screw anchor was observed. For OP and OS loading, the concrete breakout occurred in the same direction as the applied force. For IP loading, concrete breakout occurred in the support wall specimens perpendicular to the direction of the applied force.

## Summary of experimental results and comparisons with predicted capacity

A summary of the experimental results and observed failure modes is shown in Table 5. Data from each of the testing conditions were used to determine the average and standard deviation experimental capacity. In addition, the predicted

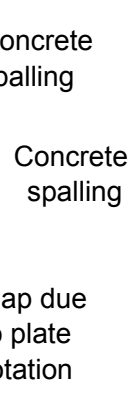


Triangular concrete breakout section  
Void filled with concrete  
Vertical crack in the bottom flange along the void  
Direction of applied load

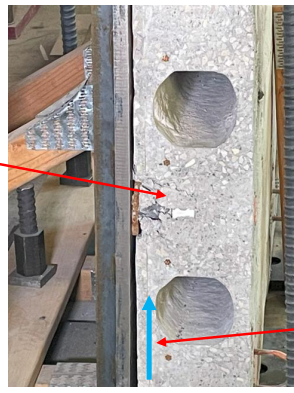
**Figure 15.** Concrete breakout failure during phase 1 out-of-plane suction testing on specimens with a 0.75 in. headed stud. Note: 1 in. = 25.4 mm.



Embedded steel plate rotation



Concrete spalling  
Gap due to plate rotation



End-face concrete spalling



Cracked PVC pipe  
Direction of applied load



Brittle PVC pipe cracking

**Figure 16.** Embedded steel plate rotation, end-face concrete spalling, and brittle polyvinyl chloride (PVC) pipe cracking during phase 1 in-plane pressure testing.

code capacity for the observed failure mode is also shown. The average experimental capacities are compared with the predicted capacity calculated for the controlling failure modes (that is, failure mode with the lowest nominal strength) according to chapter 17 of ACI 318-19<sup>1</sup> and ESR-2713.<sup>9</sup> Code predictions (detailed in the appendix to this paper) all represent the nominal capacity with no strength-reduction factor. For breakout and pryout failures in the hollow-core slab, a solid slab without voids was assumed for all calculations. The concrete for both the slab and wall was assumed to be uncracked under service conditions, in all cases, so breakout cracking factors to modify the tensile strength of anchors  $\psi_{c,N}$  were assumed to be 1.25 for the cast-in anchors in the hollow-core slab and 1.4 for the screw anchors in the walls

(section 17.6.2.5), and breakout cracking factors to modify the shear strength of anchors  $\psi_{c,V}$  were assumed to be 1.4 for all cases (section 17.7.2.5). For the IP cases, the breakout was computed for shear forces parallel to the edge, incorporating the parallel shear factor of 2 per section 17.7.2.1(c). The predicted pryout capacities for the wall contained a large reduction factor on account of the breakout splitting factor  $\psi_{cp,N}$  because the minimum edge distance in all cases was much less than the critical distance for postinstalled anchors (sections 17.6.2.6 and 17.9.5).

Results from phase 1 indicated that the shear strength of the embedded headed stud can conservatively predict the capacity of the connection in all directions. For OS loading, the observed

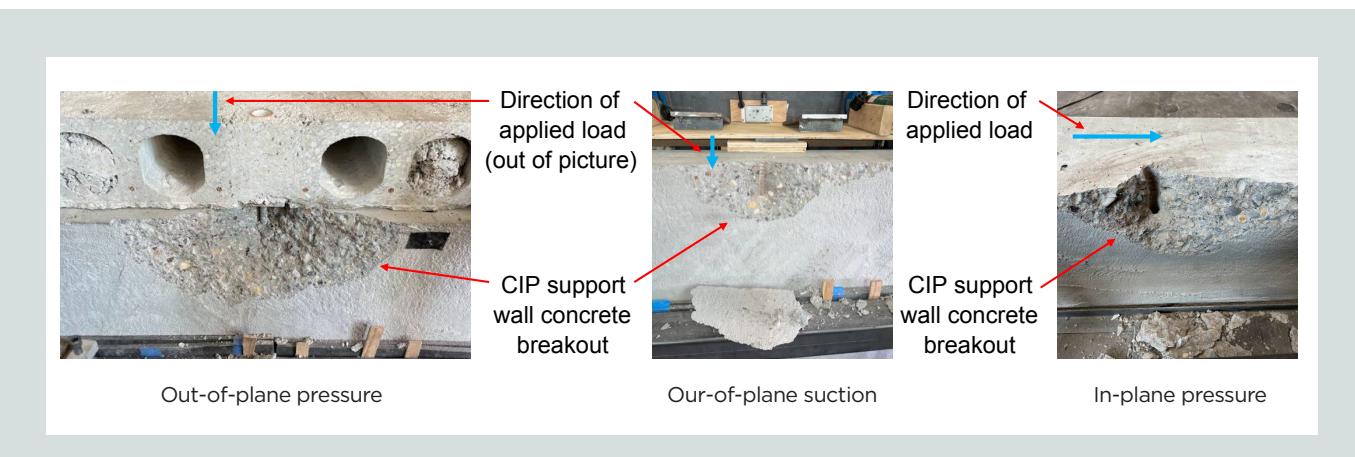


**Figure 17.** Representative concrete breakout failure in the cast-in-place (CIP) support wall during phase 2 tests with out-of-plane pressure, out-of-plane suction, and in-plane pressure loading.

**Table 5.** Summary of experimental results compared with capacity predicted using ACI 318-19

Test	Experimental results			ACI 318-19 predictions		Average experimental capacity divided by predicted capacity	
	Observed failure mode	Capacity, kip		Controlling failure mode	Capacity, kip		
		Average	Standard deviation				
P1-OP	Shearing of steel stud with steel tube weld fracture	29.6	4.8	Steel stud shear	12.0*	2.47	
P1-OS	Shearing of steel stud	11.9	2.3	Steel stud shear	12.0	0.99	
P1-OS-3/4	Hollow-core breakout	18.1	1.2	Hollow-core breakout	23.3	0.78	
P1-IP	Rotational failure about stud	17	1.2	Steel stud shear	12.0	1.42	
P2-UR-OP	Wall concrete breakout	9.8	1.6	Wall concrete prayout	6.3	1.56	
P2-R-OP	Wall concrete breakout	4.2	0.1	Wall concrete breakout	2.3	1.83	
P2-UR-OS	Wall concrete breakout	3.1	0.7	Wall concrete breakout	2.0	1.55	
P2-R-OS	Wall concrete breakout	8.6	0.9	Wall concrete prayout	6.4	1.34	
P2-UR-IP	Wall concrete breakout	13.8	2.3	Wall concrete breakout	5.9	2.34	
P2-R-IP	Wall concrete breakout	23.2	6.5	Wall concrete prayout	6.7	3.46	

Note: ACI = American Concrete Institute; IP = in-plane pressure; OP = out-of-plane pressure; OS = out-of-plane suction; P1 = phase one; P2 = phase 2; R = reinforced; UR = unreinforced. 1 kip = 4.448 kN.

\* Assuming single stud strength, thus neglecting any strength contributed by the steel tube.

capacity was nearly equal to the capacity of a single headed stud in shear because the steel tube did not have enough concrete cover to effectively bear load in this direction. However, for OP loading, the steel tube appeared to carry a large portion of the applied load, as indicated by the increased capacity that

still ultimately resulted in a steel shearing failure. The mechanism observed for IP loading, rotation of the embedded assembly about the headed stud, does not match with any specific mechanism in ACI 318-19. For this load case, code results for concrete breakout of a single headed stud with eccentric

loading parallel to the edge estimated a capacity of 26.7 kip (119 kN), overpredicting the failure capacity, while shear failure of the steel stud underpredicted the capacity. Concrete breakout failure in the hollow-core slab was only achieved by increasing the stud diameter to 0.75 in. (19 mm), though in this case the ACI 318-19 breakout capacity was approximately 30% greater than the observed capacity. This was likely on account of the voids in the slab because the predicted capacity was computed assuming a solid slab. Subtracting the void area from the projected concrete shear failure area  $A_{Vc}$  (section 17.7.2.1.1) results in a predicted breakout capacity of 16.8 kip (74.9 kN), which underestimates the observed capacity by only 7%.

Results from testing the slab-to-wall subassemblies in phase 2 were most representative of the loading that this connection will experience in a constructed building. Data in Table 5 indicate that all slab-to-wall subassemblies failed at an applied load higher than that predicted by ACI 318-19,<sup>1</sup> with a ratio of average experimental capacity divided by capacity predicted with ACI 318-19 that ranged from 1.34 to 3.46. Concrete pryout was the code-predicted failure mode for tests with larger edge distances, though these distances were still much less than the critical distance for postinstalled anchors. No pryout failures were observed in testing. Regardless, the observed experimental capacities were still greater than the code-predicted concrete breakout capacities for these three cases: 7.9, 7.4, and 11.6 kip (35.2, 32.9 kN, and 51.7 kN) for P2-UR-OP, P2-R-OS, and P2-R-IP, respectively. The observed capacity in IP loading was consistently the most underestimated by the code, even when accounting for the parallel shear factor of 2 for breakout failures with loading parallel to the edge. Failure modes observed during phase 1 testing of the connection assembly, such as steel tube weld fracture, steel stud shear failure, and plastic coupler cracking failure, did not affect the wall subassemblies. Thus, modifications to the connection assembly, such as using a larger steel shear stud or increasing the size of the weld around the steel tube, could be completed, but the changes may not affect the overall connection capacity. **Table 6** compares the experimental results from this study with those from SMA<sup>5</sup> and Brito et al.<sup>6</sup> The connection proposed herein always resulted in a concrete failure in the wall, never an anchor failure, which contrasts with results from the previous dowel connection studies.

**Table 6.** Comparison of experimental results from this research study with those from Spancrete Manufacturers' Association and Brito et al.

Bearing condition	Loading direction	Failure load, kip			
		SMA	Brito et al. (dry fit)	Connection assembly investigated herein	
				Unreinforced walls	Reinforced walls
End bearing	OP	3.40	5.6	9.8	4.2
	OS	2.78	2.1	3.1	8.6
	IP	4.50	5.8	13.8	23.2

Sources: Spancrete Manufacturers' Association (2010); Brito et al. (2022).

Note: IP = in-plane pressure; OP = out-of-plane pressure; OS = out-of-plane suction; SMA = Spancrete Manufacturers' Association (2010). 1 kip = 4.448 kN.

## Conclusion

A new slab-to-wall connection assembly that consisted of a steel plate and stud embedded in the void of a hollow-core slab was investigated in this study. During phase 1, the capacity of the connection assembly embedded in a hollow-core slab was established by directly subjecting the assembly to OP, OS, and IP loading until steel or concrete failure. During phase 2, slab-to-wall subassembly testing was conducted on hollow-core slabs anchored to the tops of cast-in-place support walls to characterize performance of the connection assembly when OP, OS, or IP loading was applied. The following conclusions were drawn based on observations and data gathered during this research program:

- The proposed connection assembly requires no field welding and allows for all components but the final screw anchor to be assembled and aligned in the precasting plant.
- Failure modes observed during phase 1 testing of the connection assembly, such as steel tube weld fracture, steel stud shear failure, and plastic coupler cracking failure, did not affect the phase 2 subassembly test results. Minor modifications to the connection assembly during fabrication likely would not affect the overall connection capacity, which is controlled by concrete breakout of the wall.
- Failure loads during phase 1 connection assembly testing were conservative compared with those predicted by ACI 318-19.<sup>1</sup> The capacity on the hollow-core side of the connection could always be conservatively estimated as the shear capacity of a single headed stud.
- Concrete breakout of the supporting cast-in-place wall was the sole failure mode observed during phase 2 slab-to-wall subassembly testing. Results from this phase were most representative of the loading and behavior that this connection assembly would experience in a constructed building.
- Failure loads during phase 2 subassembly testing were conservative compared with those predicted by ACI 318-19, with a ratio of average experimental

failure load to predicted code capacity that ranged from 1.34 to 3.46.

## Recommendations

The following recommendations were formed based on the results of this research program:

- During fabrication of the connection assembly, securing the steel tube to the embedded plate with an all-around weld rather than individual welds on two sides of the tube would likely prevent weld fracture and increase the OP failure load. However, fracture of the two-side weld was not observed in the slab-to-wall subassembly testing and would have no effect on the overall connection capacity, which is controlled by breakout of the wall.
- During fabrication of the connection assembly, the use of a 0.75 in. (19 mm) diameter shear stud rather than a 0.5 in. (12.7 mm) diameter stud led to the failure mode of hollow-core concrete breakout during tests with OS loading. However, shearing of the 0.5 in. diameter steel stud was not observed in the slab-to-wall subassembly testing. A 0.5 in. diameter steel stud is recommended due to reduced cost and no adverse effects observed during subassembly testing.
- During connection assembly testing with IP loading, the principal failure mode involved rotation of the embedded plate and brittle cracking of the PVC coupler. However, this failure mode was not observed in the slab-to-wall subassembly testing; contact between the hollow-core slab and support wall likely restricted plate rotation during subassembly testing during IP loading. Use of the PVC coupler and pipe is recommended to ensure easy access to the predrilled hole during postinstallation of the screw anchor.
- Overall, testing of the slab-to-wall subassemblies showed that predicted capacities using chapter 17 of ACI-318-19<sup>1</sup> were conservative, and the end-bearing performance of the embedded steel plate and stud connection assembly during these tests was adequate. It is recommended that this connection assembly be implemented in slab-to-wall connections and that the engineer of record apply an appropriate safety factor to the capacity based on the 5% fractile and engineering judgement.

## Acknowledgments

The authors would like to acknowledge the generous donations of time, materials, and full-scale specimens from Molin Concrete Products.

## References

1. ACI (American Concrete Institute) Committee 318. 2019. *Building Code Requirements for Structural Concrete (ACI 318-19) and Commentary (ACI 318R-19)*. Farmington Hills, MI: ACI.
2. Clementi, F., A. Scalbi, and S. Lenci. 2016. "Seismic Performance of Precast Reinforced Concrete Buildings with Dowel Pin Connections." *Journal of Building Engineering*, no. 7, 224–238. <https://doi.org/10.1016/j.jobe.2016.06.013>.
3. Engström, B., S. Alexander, A. Cholewicki, et al. 2008. *Structural Connections for Precast Concrete Buildings: Guide to Good Practice*. Bulletin 43. Lausanne, Switzerland: fib (International Federation for Structural Concrete). <https://doi.org/10.35789/fib.BULL.0043>.
4. PCI Hollow Core Slab Producers Committee. 2015. *PCI Manual for the Design of Hollow Core Slabs and Walls*. MNL-126. 3rd ed. Chicago, IL: PCI. <https://doi.org/10.15554/MNL-126-15>.
5. Spancrete Manufacturers' Association. 2010. "Dowel Connections." Research note 1015.
6. Brito, S. H., K. Mahmoud, K. Truderung, and E. El-Salakawy. 2022. "Behavior of Reinforcing Bar Connections of Hollow-Core Slabs to Masonry Walls Under In-Plane Forces." *PCI Journal* 67 (6): 51–68. <https://doi.org/10.15554/pcij67.6-03>.
7. AISC (American Institute of Steel Construction). 2023. *Steel Construction Manual*. 16th ed. Chicago, IL: AISC.
8. Jackman, K. 2023. "Embedded Plate Connection Between Hollow-Core Slabs and Concrete Walls." MS thesis, University of Minnesota Duluth. <https://hdl.handle.net/11299/259544>.
9. ICC Evaluation Service. 2025. ICC-ES Evaluation Report ESR-2713. <https://www.icc-es.org/wp-content/uploads/report-directory/ESR-2713.pdf>.

## Notation

$A_{vc}$  = projected concrete failure area of a single anchor or group of anchors for calculation of strength in shear

$\psi_{cp,N}$  = breakout splitting factor used to modify tensile strength of postinstalled anchors intended for use in uncracked concrete without supplementary reinforcement to account for the splitting tensile stresses

$\psi_{c,N}$  = breakout cracking factor used to modify tensile strength of anchors based on the influence of cracks in concrete

$\psi_{c,V}$  = breakout cracking factor used to modify shear strength of anchors based on the influence of cracks in concrete and presence or absence of supplementary reinforcement

## About the authors



Kal Jackman is a structural engineer at BKBM Engineers in Minneapolis, Minn. He received his BS and MS in civil engineering from the University of Minnesota Duluth.



Ben Dymond, PhD, is an associate professor in the Department of Civil Engineering, Construction Management, and Environmental Engineering at Northern Arizona University and the director of the PCI Foundation program

Innovative Building Technology in a Precast Concrete Curriculum. His research interests include design and analysis of concrete structural systems and their components, destructive experimental investigations, short-term field monitoring experiments, and engineering education.



Brock Hedegaard, PhD, PE, is an associate professor in the Department of Civil Engineering at the University of Minnesota Duluth. His research interests include modeling time-dependent processes of concrete, behavior of frames under large displacements, and data analytics for structural health monitoring.

## Abstract

Currently, hollow-core slabs are connected to walls using dowel or welded connections. The existing research on these connections is minimal, and their design capacity is limited. This research project investigated a new slab-to-wall end-bearing connection assembly that consisted of a steel plate and stud embedded in a hollow-core slab void. The capacity of the connection assembly embedded in a hollow-core slab was established by directly loading the assembly until steel or concrete failure. Results indicated that the connection assembly had conservative failure loads compared with predicted values for load applied in various directions. Slab-to-wall subassembly testing was conducted on hollow-core slabs anchored to the tops of cast-in-place walls. The setup was representative of the loading and behavior that this connection assembly would experience in a constructed build-

ing. Capacity of the subassembly was established by applying load until the hollow-core slab, wall, or anchor failed. The subassembly results indicated that the wall failed first in concrete breakout. Experimental capacities were conservative compared with capacities predicted using the American Concrete Institute's *Building Code Requirements for Structural Concrete (ACI 318-19) and Commentary (ACI 318R-19)*. The combined results from this experimental program indicated that the proposed embedded steel plate and stud connection assembly had sufficient capacity and was easy to install.

## Keywords

Cast-in-place, embed plate, end bearing, hollow-core, in plane, lateral load, out of plane, pressure, screw anchor, slab, steel stud, suction.

## Review policy

This paper was reviewed in accordance with the Precast/Prestressed Concrete Institute's peer-review process. The Precast/Prestressed Concrete Institute is not responsible for statements made by authors of papers in *PCI Journal*. No payment is offered.

## Publishing details

This paper appears in *PCI Journal* (ISSN 0887-9672) V. 71, No. 2, March–April 2026, and can be found at <https://doi.org/10.15554/pcij71.2-01>. *PCI Journal* is published bimonthly by the Precast/Prestressed Concrete Institute, 8770 W. Bryn Mawr Ave., Suite 1150, Chicago, IL 60631. Copyright © 2026, Precast/Prestressed Concrete Institute.

## Reader comments

Please address any reader comments to journal@pci.org or Precast/Prestressed Concrete Institute, c/o *PCI Journal*, 8770 W. Bryn Mawr Ave., Suite 1150, Chicago, IL 60631.

# Appendix: Embedded plate connection between hollow-core slabs and concrete walls

Kal A. Jackman, Benjamin Z. Dymond, and Brock D. Hedegaard

## Calculation tables for predicted capacity

This appendix contains additional tables for “Embedded Plate Connection between Hollow-core Slabs and Concrete Walls,” by Kal A. Jackman, Benjamin Z. Dymond, and Brock D. Hedegaard.

**Tables A.1** through **A.5** list all known or calculated variables used to generate the following predicted capacities:

- cast-in headed stud and postinstalled anchor shear capacity
- concrete breakout and prout failures of the hollow-core specimens
- concrete breakout and prout failures of the wall specimens

**Table A.1.** Headed stud and anchor shear capacity

Anchor type	Cast-in headed stud		Postinstalled anchors
	0.5 in.	0.75 in.	
$A_{seV}$ , in.2	0.196	0.442	0.183*
$f_{uta}$ , psi	61,000 <sup>†</sup>	61,000 <sup>†</sup>	110,000 <sup>†</sup>
$V_{sa}$ , lb	11,977	26,949	12,078

Note:  $A_{seV}$  = effective cross-sectional area of anchor in shear;  $f_{uta}$  = specified tensile strength of anchor, shall not exceed  $1.9f_{y0}$  or 125,000 psi;  $f_{y0}$  = specified yield strength of anchor;  $V_{sa}$  = nominal shear strength of a single anchor as governed by the steel strength. 1 in. = 25.4 mm; 1 in.<sup>2</sup> = 645.2 mm<sup>2</sup>; 1 lb = 4450 kN; 1 psi = 6.895 kPa.

\* Value from ICC Evaluation Service (2025), Table 1A.

<sup>†</sup> Assumed type A.

**Table A.2.** Phase 1: Concrete breakout failure of the hollow-core specimens

Test	$h_{ef}$ , in.	$c_{a1}$ , in.	$c_{a2}$ , in.	$A_{Vco}$ , in. <sup>2</sup>	$h_a$ , in.	$A_{vc}$ , in. <sup>2</sup>	$d_a$ , in.	$\lambda_a$	$f'_c$ , psi	$V_b$ , lb	$\psi_{ed,V}$	$\psi_{c,V}$	$\psi_{h,V}$	$\psi_{ec,V}$	$V_{cb}$ , lb
OS-1/2	4	8.5	19	325	8	204	0.5	1	9590	18,207	1	1.4	1.262	1	20,191
OS-3/4	4	8.5	19	325	8	204	0.75	1	10,714	20,997	1	1.4	1.262	1	23,285
OP	4	39.5	19	722	8	304	0.5	1	9927	33,698	1	1.4	1.541	1	30,612
IP	4	8.5	19	325	8	204	0.5	1	9927	18,524	1	1.4	1.262	0.65	26,685
IP	4	8.5	19	325	8	204	0.5	1	9927	18,524	1	1.4	1.262	0.787	32,355

Note:  $A_{vc}$  = projected concrete failure area of a single anchor or group of anchors for calculation of strength in shear;  $A_{Vco}$  = projected concrete failure area of a single anchor, for calculation of strength in shear, if not limited by corner influences, spacing, or member thickness;  $c_{a1}$  = distance from the center of an anchor shaft to the edge of concrete in one direction;  $c_{a2}$  = distance from center of an anchor shaft to the edge of concrete in the direction perpendicular to  $c_{a1}$ ;  $d_a$  = outside diameter of anchor or shaft diameter of headed stud;  $f'_c$  = specified compressive strength of concrete;  $h_a$  = thickness of member in which an anchor is located, measured parallel to anchor axis;  $h_{ef}$  = effective embedment depth of anchor; IP = in-plane pressure; OP = out-of-plane pressure; OS = out-of-plane suction;  $V_b$  = basic concrete breakout strength in shear of a single anchor in cracked concrete;  $V_{cb}$  = nominal concrete breakout strength in shear of a single anchor;  $\lambda_a$  = modification factor to reflect the reduced mechanical properties of lightweight concrete in certain concrete anchorage applications;  $\psi_{c,V}$  = breakout cracking factor used to modify shear strength of anchors based on the influence of cracks in concrete and presence or absence of supplementary reinforcement;  $\psi_{ec,V}$  = breakout eccentricity factor used to modify shear strength of anchors based on eccentricity of applied loads;  $\psi_{ed,V}$  = breakout edge effect factor used to modify shear strength of anchors based on proximity to edges of concrete member;  $\psi_{h,V}$  = breakout thickness factor used to modify shear strength of anchors located in concrete members with  $h_a < 1.5c_{a1}$ ; 1 in. = 25.4 mm; 1 in.<sup>2</sup> = 645.2 mm<sup>2</sup>; 1 lb = 4450 kN; 1 psi = 6.895 kPa.

**Table A.3.** Phase 1: Concrete prout failure of the hollow-core specimens

Test	$h_{nom}$ , in.	$k_{cp}$	$h_{ef}$ , in.	$A_{Nco}$ , in. <sup>2</sup>	$c_{a1}$ , in.	$c_{a2}$ , in.	$A_{Nc}$ , in. <sup>2</sup>	$k_c$	$\lambda_a$	$f'_c$ , psi	$N_b$ , lb	$\psi_{ed,N}$	$\psi_{c,N}$	$c_{a,min}$ , in.	$\psi_{cp,N}$	$N_{cp}$ , lb	$V_{cp}$ , lb
OS-1/2	4	2	4	144	8.5	>1.5 $c_{a1}$	144	24	1	9590	18,802	1	1.25	8.5	1	23,503	47,005
OS-3/4	4	2	4	144	8.5	>1.5 $c_{a1}$	144	24	1	10,714	19,200	1	1.25	8.5	1	24,000	48,000
OP	4	2	4	144	39.5	>1.5 $c_{a1}$	144	24	1	9927	19,130	1	1.25	8.5	1	23,913	47,825
IP	4	2	4	144	8.5	>1.5 $c_{a1}$	144	24	1	9927	19,130	1	1.25	8.5	1	23,913	47,825

Note:  $A_{Nc}$  = projected concrete failure area of a single anchor for calculations of strength in tension;  $A_{Nco}$  = projected concrete failure area of a single anchor for calculation of strength in tension if not limited by corner influence, spacing, or member thickness;  $A_{vc}$  = projected concrete failure area of a single anchor or group of anchors for calculation of strength in shear;  $c_{a1}$  = distance from the center of an anchor shaft to the edge of concrete in one direction;  $c_{a2}$  = distance from center of an anchor shaft to the edge of concrete in the direction perpendicular to  $c_{a1}$ ;  $c_{a,min}$  = minimum distance from center of an anchor shaft to the edge of concrete;  $f'_c$  = specified compressive strength of concrete;  $h_{ef}$  = effective embedment depth of anchor;  $h_{nom}$  = nominal embedment depth of anchor; IP = in-plane pressure;  $k_c$  = coefficient for basic concrete breakout strength in tension, equal to 17 for postinstalled anchors;  $k_{cp}$  = coefficient of prout strength, equal to 1.0 for  $h_{ef} < 2.5$  in. and 2.0 for  $h_{ef} \geq 2.5$  in.;  $N_b$  = basic concrete breakout strength in shear of a single anchor in cracked concrete;  $N_{cp}$  = basic concrete prout strength of a single anchor; OP = out-of-plane pressure; OS = out-of-plane suction;  $V_{cp}$  = nominal concrete prout strength of a single anchor;  $\lambda_a$  = modification factor to reflect the reduced mechanical properties of lightweight concrete in certain concrete anchorage applications;  $\psi_{c,N}$  = breakout cracking factor used to modify tensile strength of anchors based on the influence of cracks in concrete;  $\psi_{cp,N}$  = breakout splitting factor used to modify tensile strength of postinstalled anchors intended for use in uncracked concrete without supplementary reinforcement to account for the splitting tensile stresses;  $\psi_{ed,N}$  = breakout edge effect factor used to modify tensile strength of anchors based on proximity to edges of concrete member. 1 in. = 25.4 mm; 1 in.<sup>2</sup> = 645.2 mm<sup>2</sup>; 1 lb = 4450 kN; 1 psi = 6.895 kPa.

**Table A.4.** Phase 2: Concrete breakout failure of the wall specimens

Test	$h_{ef}$ , in.	$c_{a1}$ , in.	$c_{a2}$ , in.	$h_a$ , in.	$d_a$ , in.	$\lambda_a$	$f'_c$ , psi	$\psi_{  }$	$\psi_{ed,V}$	$\psi_{c,V}$	$\psi_{h,V}$	$V_b$ , lb	$V_{cb}$ , lb
OS-UR-1	4.5	1.875	$>1.5c_{a1}$	38	0.5	1	5146	1	1	1.4	1	1382	1935
OS-UR-2	4.5	2	$>1.5c_{a1}$	38	0.5	1	5146	1	1	1.4	1	1522	2131
OS-UR-3	4.5	1.875	$>1.5c_{a1}$	38	0.5	1	5146	1	1	1.4	1	1382	1935
OS-R-1	4.5	4.25	$>1.5c_{a1}$	38	0.5	1	5436	1	1	1.4	1	4846	6784
OS-R-2	4.5	4.875	$>1.5c_{a1}$	38	0.5	1	5436	1	1	1.4	1	5954	8336
OS-R-3	4.5	4.375	$>1.5c_{a1}$	38	0.5	1	5436	1	1	1.4	1	5062	7087
OP-UR-1	4.5	4.75	$>1.5c_{a1}$	38	0.5	1	5436	1	1	1.4	1	5726	8016
OP-UR-2	4.5	4.875	$>1.5c_{a1}$	38	0.5	1	5436	1	1	1.4	1	5934	8308
OP-UR-3	4.5	4.5	$>1.5c_{a1}$	38	0.5	1	5436	1	1	1.4	1	5280	7392
OP-R-1	4.5	2	$>1.5c_{a1}$	38	0.5	1	5436	1	1	1.4	1	1565	2191
OP-R-2	4.5	2	$>1.5c_{a1}$	38	0.5	1	5436	1	1	1.4	1	1565	2191
OP-R-3	4.5	2.125	$>1.5c_{a1}$	38	0.5	1	5436	1	1	1.4	1	1713	2398
IP-UR-1	4.5	2.25	$>1.5c_{a1}$	16	0.5	1	5800	2	1	1.4	1	1928	5400
IP-UR-2	4.5	2.5	$>1.5c_{a1}$	16	0.5	1	5800	2	1	1.4	1	2259	6324
IP-UR-3	4.5	2.375	$>1.5c_{a1}$	16	0.5	1	5800	2	1	1.4	1	2091	5856
IP-R-1	4.5	3.75	$>1.5c_{a1}$	16	0.5	1	5800	2	1	1.4	1	4149	11,617
IP-R-2	4.5	3.75	$>1.5c_{a1}$	16	0.5	1	5800	2	1	1.4	1	4149	11,617
IP-R-3	4.5	3.75	$>1.5c_{a1}$	16	0.5	1	5800	2	1	1.4	1	4149	11,617

Note:  $c_{a1}$  = distance from the center of an anchor shaft to the edge of concrete in one direction;  $c_{a2}$  = distance from center of an anchor shaft to the edge of concrete in the direction perpendicular to  $c_{a1}$ ;  $d_a$  = outside diameter of anchor or shaft diameter of headed stud;  $f'_c$  = specified compressive strength of concrete;  $h_a$  = thickness of member in which an anchor is located, measured parallel to anchor axis;  $h_{ef}$  = effective embedment depth of anchor; IP = in-plane pressure; OP = out-of-plane pressure; OS = out-of-plane suction; R = reinforced; UR = unreinforced;  $V_b$  = basic concrete breakout strength in shear of a single anchor in cracked concrete;  $V_{cb}$  = nominal concrete breakout strength in shear of a single anchor;  $V_{cbg}$  =  $\lambda_a$  = modification factor to reflect the reduced mechanical properties of lightweight concrete in certain concrete anchorage applications;  $\psi_{c,V}$  = breakout cracking factor used to modify shear strength of anchors based on the influence of cracks in concrete and presence or absence of supplementary reinforcement;  $\psi_{ed,V}$  = breakout edge effect factor used to modify shear strength of anchors based on proximity to edges of concrete member;  $\psi_{h,V}$  = breakout thickness factor used to modify shear strength of anchors located in concrete members with  $h_a < 1.5c_{a1}$ ;  $\psi_{||}$  = author-defined symbol for the factor used to double the value of  $V_{cb}$  or  $V_{cbg}$  when shear is parallel to an edge per section 17.7.2.1(c) of ACI 318-19; 1 in. = 25.4 mm; 1 lb = 4450 kN; 1 psi = 6.895 kPa.

**Table A.5.** Phase 2: Concrete prayout failure of the wall specimens

Test	$h_{nom}$ , in.	$k_{cp}$	$h_{ef}$ , in.	$A_{Nco}$ , in. <sup>2</sup>	$c_{a1}$ , in.	$c_{a2}$ , in.	$A_{Nc}$ , in. <sup>2</sup>	$k_c$	$\lambda_a$	$f'_c$ , psi	$N_b$ , lb	$\psi_{ed,N}$	$\psi_{c,N}$	$c_{ac}$ , in.	$c_{a,min}$ , in.	$\psi_{cp,N}$	$N_{cp}$ , lb	$V_{cp}$ , lb
OS-UR-1	4.5	2	4.5	182	1.875	>1.5 $c_{a1}$	108	17	1	5146	11,641	0.783	1.4	18	1.875	0.375	2836	5674
OS-UR-2	4.5	2	4.5	182	2	>1.5 $c_{a1}$	108	17	1	5146	11,641	0.789	1.4	18	2	0.375	2857	5715
OS-UR-3	4.5	2	4.5	182	1.875	>1.5 $c_{a1}$	108	17	1	5146	11,641	0.783	1.4	18	1.875	0.375	2836	5674
OS-R-1	4.5	2	4.5	182	4.25	>1.5 $c_{a1}$	108	17	1	5436	11,965	0.867	1.4	18	3.75	0.375	3226	6453
OS-R-2	4.5	2	4.5	182	4.875	>1.5 $c_{a1}$	108	17	1	5436	11,965	0.839	1.4	18	3.125	0.375	3122	6245
OS-R-3	4.5	2	4.5	182	4.375	>1.5 $c_{a1}$	108	17	1	5436	11,965	0.861	1.4	18	3.625	0.375	3206	6411
OP-UR-1	4.5	2	4.5	182	4.75	>1.5 $c_{a1}$	108	17	1	5436	11,965	0.844	1.4	18	3.25	0.375	3143	6287
OP-UR-2	4.5	2	4.5	182	4.875	>1.5 $c_{a1}$	108	17	1	5436	11,965	0.839	1.4	18	3.125	0.375	3122	6245
OP-UR-3	4.5	2	4.5	182	4.5	>1.5 $c_{a1}$	108	17	1	5436	11,965	0.856	1.4	18	3.5	0.375	3185	6370
OP-R-1	4.5	2	4.5	182	2	>1.5 $c_{a1}$	108	17	1	5436	11,965	0.789	1.4	18	2	0.375	2937	5873
OP-R-2	4.5	2	4.5	182	2	>1.5 $c_{a1}$	108	17	1	5436	11,965	0.789	1.4	18	2	0.375	2937	5873
OP-R-3	4.5	2	4.5	182	2.125	>1.5 $c_{a1}$	108	17	1	5436	11,965	0.794	1.4	18	2.125	0.375	2957	5915
IP-UR-1	4.5	2	4.5	182	2.25	>1.5 $c_{a1}$	108	17	1	5800	12,359	0.800	1.4	18	2.25	0.375	3076	6152
IP-UR-2	4.5	2	4.5	182	2.5	>1.5 $c_{a1}$	108	17	1	5800	12,359	0.811	1.4	18	2.5	0.375	3119	6237
IP-UR-3	4.5	2	4.5	182	2.375	>1.5 $c_{a1}$	108	17	1	5800	12,359	0.806	1.4	18	2.375	0.375	3097	6195
IP-R-1	4.5	2	4.5	182	3.75	>1.5 $c_{a1}$	108	17	1	5800	12,359	0.867	1.4	18	3.75	0.375	3332	6664
IP-R-2	4.5	2	4.5	182	3.75	>1.5 $c_{a1}$	108	17	1	5800	12,359	0.867	1.4	18	3.75	0.375	3332	6664
IP-R-3	4.5	2	4.5	182	3.75	>1.5 $c_{a1}$	108	17	1	5800	12,359	0.867	1.4	18	3.75	0.375	3332	6664

Note:  $A_{Nc}$  = projected concrete failure area of a single anchor for calculations of strength in tension;  $A_{Nco}$  = projected concrete failure area of a single anchor for calculation of strength in tension if not limited by corner influence, spacing, or member thickness;  $c_{a1}$  = distance from the center of an anchor shaft to the edge of concrete in one direction;  $c_{a2}$  = distance from center of an anchor shaft to the edge of concrete in the direction perpendicular to  $c_{a1}$ ;  $c_{ac}$  = critical edge distance required to develop the basic strength as controlled by concrete breakout or bond of a postinstalled anchor in tension in uncracked concrete without supplementary reinforcement to control splitting;  $c_{a,min}$  = minimum distance from center of an anchor shaft to the edge of concrete;  $f'_c$  = specified compressive strength of concrete;  $h_{ef}$  = effective embedment depth of anchor;  $h_{nom}$  = nominal embedment depth of anchor; IP = in-plane pressure;  $k_c$  = coefficient for basic concrete breakout strength in tension, equal to 17 for postinstalled anchors;  $k_{cp}$  = coefficient of prayout strength, equal to 1.0 for  $h_{ef} < 2.5$  in. and 2.0 for  $h_{ef} \geq 2.5$  in.;  $N_b$  = basic concrete breakout strength in shear of a single anchor in cracked concrete;  $N_{cp}$  = basic concrete prayout strength of a single anchor; OP = out-of-plane pressure; OS = out-of-plane suction; R = reinforced; UR = unreinforced;  $V_{cp}$  = nominal concrete prayout strength of a single anchor;  $\lambda_a$  = modification factor to reflect the reduced mechanical properties of lightweight concrete in certain concrete anchorage applications;  $\psi_{c,N}$  = breakout cracking factor used to modify tensile strength of anchors based on the influence of cracks in concrete;  $\psi_{cp,N}$  = breakout splitting factor used to modify tensile strength of postinstalled anchors intended for use in uncracked concrete without supplementary reinforcement to account for the splitting tensile stresses;  $\psi_{ed,N}$  = breakout edge effect factor used to modify tensile strength of anchors based on proximity to edges of concrete member. 1 in. = 25.4 mm; 1 in.<sup>2</sup> = 645.2 mm<sup>2</sup>; 1 lb = 4450 kN; 1 psi = 6.895 kPa.